Cytometry PART A
Journal of the International Society for Advancement of Cytometry

MIFlowCyt

Physics of a Rapid CD4 Lymphocyte Count with Colloidal Gold

P. Hansen,[1*] D. Barry,[2] A. Restell,[2] D. Sylvia,[2] O. Magnin,[3] D. Dombkowski,[4] F. Preffer[4]

[1]UBT Inc., Canaan, New York

[2]PointCare Technologies Inc., Marlborough, Massachusetts

[3]C2 Diagnostics, Montpellier, France

[4]Department of Pathology, Massachusetts General Hospital, Boston, Massachusetts

Received 22 March 2011; Revision Received 11 August 2011; Accepted 12 August 2011

Additional Supporting Information (MIFlowCyt item location) may be found in the online version of this article.

*Correspondence to: P. Hansen, Union Biometrica Technology Inc., 121 Top of Dean Hill Rd, PO 315, Canaan, NY 12029, USA

Email: phansen5488@gmail.com

Published online 00 Month 2011 in Wiley Online Library (wileyonlinelibrary.com)

DOI: 10.1002/cyto.a.21139

Abstract

The inherent surface charges and small diameters that confer colloidal stability to gold particle conjugates (immunogold) are detrimental to rapid cell surface labeling and distinct cluster definition in flow cytometric light scatter assays. Although the inherent immunogold surface charge prevents self aggregation when stored in liquid suspension, it also slows binding to cells to timeframes of hours and inhibits cell surface coverage. Although the small diameter of immunogold particles prevents settling when in liquid suspension, small particles have small light scattering cross sections and weak light scatter signals. We report a new, small particle lyophilized immunogold reagent that maintains activity after 42°C storage for a year and can be rapidly dissolved into stable liquid suspension for use in labelling cells with larger particle aggregates that have enhanced scattering cross section. Labeling requires less than 1 min at 20°C, which is ~30 times faster than customary fluorescent antibody labeling. The labeling step involves neutralizing the surface charge of immunogold and creating specifically bound aggregates of gold on the cell surface. This process provides distinct side-scatter cluster separation with blue laser light at 488 nm, which is further improved by using red laser light at 640 nm. Similar comparisons using LED light sources showed less improvement with red light, thereby indicating that coherent light scatter is of significance in enhancing side-scatter cluster separation. The physical principles elucidated here for this technique are compatible with most flow cytometers; however, future studies of its clinical efficacy should be of primary interest in point-of-care applications where robust reagents and rapid results are important.

Key terms

CD4 lymphocytes; nanoparticles; point of care; light scatter; cytometry

FLOW cytometry is the recognized clinical standard by which human T-cell subclasses are enumerated in HIV-infected patients. Bringing this standard to resource poor environments requires simplified instrumentation, robust reagents, and rapid test results. This report investigates light scatter as a simplification for flow cytometry instrumentation, immunogold as a robust reagent, and a novel cationic surfactant to speed immunogold binding to cell surface antigens, thus potentially providing CD4 T-cell results to patients in minutes without the need for a return visit.

The potential for simplification offered by light scatter detection of immunogold conjugates of monoclonal antibodies has attracted attention for more than 2 decades. In 1984, Bohmer and King (1) reported immunogold labelling of mouse spleen lymphocytes. They were unable to achieve useful side scatter cluster separation with an argon laser operating at several wavelengths from 451.7 nm to 528.9 nm but were able to achieve side scatter cluster separation with a HeNe laser at 632.8 nm. The impractical feature of their assay was that to overcome very long incubation times, three 5 min centrifugation and resuspension steps were needed. In 1987, Festin et al. (2) reported successful immunogold labeling and side scatter detection of human T lymphocytes with 40-nm gold colloids using an argon laser at 488 nm. Festin et al. also found it necessary to repeatedly centrifuge and resuspend the sample to bind the

ISAC
International Society for Advancement of Cytometry

immunogold to cells. About a decade later, Siiman et al. reported another approach where large polystyrene beads of ~2 μ diameter were coated with either metallic (electrically neutral) silver or gold nanoparticles and conjugated with monoclonal antibodies. Experiments with gold-coated polystyrene particle conjugates using CD4 antibodies were carried out at 633 nm with better cluster separation than with silver nanoparticles (3). However, free polystyrene conjugate particles interfered with the CD4+ lymphocyte cluster on side scatter making cell counting difficult. The method of Siiman et al. used a 10 min centrifugation process to prepare white cell buffy coat samples and 2 min of mixing by nutation to bind the polystyrene conjugates to cells. Siiman et al. noted that they were unsuccessful in creating side scatter clusters with nanoparticles smaller than 50 nm and speculated that other reports of side scatter cluster separation with 40-nm gold particles may have been the result of accidental particle aggregation. More recently, Crow et al. have reported the use of 30 nm rod-shaped immunogold particles in a cellular assay (4). The method uses 20 min of vortex mixing. Distinct dot plot clusters were obtained with a 633 nm laser but not so with a 488 nm laser.

Building on these prior studies, this report describes an 80-nm-diameter particle immunogold flow cytometric assay for CD4+ lymphocytes that produces distinct CD4+ and CD4− cell clusters, requires no centrifugation, and needs less than a minute for complete sample preparation including labeling and red cell lysis. The immunogold reagent is stable in real time for 1 year at 42°C but nonetheless able to bind to CD4+ lymphocytes in 45 s at room temperature.

There are three physical-chemical principles that form the foundation for the simplified and rapid immunogold cell surface labeling assay for CD4+ lymphocytes reported here. The first involves the deliberate chemical destruction of colloidal stability of the immunogold conjugate during the cell labeling step which gives rise to an accelerated antigen binding reaction rate, and the formation of gold particle aggregates around the CD4 antigenic sites. The second is resonant surface mode behavior of the aggregates which favors the use of far red light near 640 nm for enhanced cluster separation. The third is the optically coherent reinforcement of side scatter which is caused by the dimensions of these aggregates and is mathematically related to Bragg scatter.

Materials and Methods

Cell Preparation and Fluorescence Flow Cytometry

Peripheral blood from healthy donors collected between September 2010 and February 2011 was drawn into K2EDTA Vacutainer™ tubes (BD Biosciences, San Jose, CA) kept at room temperature (20°C) and used in these experiments within 5 h. Whole blood was stained with tittered volumes of CD45-FITC (15 μl), CD3-APC (5 μl), and CD4-PE/CY7 (7 μl) (BD Biosciences) for 15 min at room temperature. Blood was lysed for 10 min with BD Lysing Buffer, washed with PBS, and fixed with PBS 1% paraformaldehyde. These cells were analyzed on an LSR ll flow cytometer (BD Biosciences) equipped with air-cooled lasers having adjustable output power control (5). Eight peak rainbow calibration particles (RCP-30-5A; Spherotech, Inc., Lake Forest, IL) were used as a quality control measure to calibrate the LSR II flow cytometer and to check alignment and sensitivity of scatter and fluorescent signals to all detectors. Data were collected with DIVA 6.1 software (BD Biosciences) with 488 nm at 100 mW and 640 nm at 80 mW lasers. CD4+ cells were identified by gating lymphocytes with a combination of 90 degree side scatter (SSC) and forward angle light scatter (FSC) in addition to CD45+ and CD3+ expression. The plane of polarization for both the 448 nm and 640 nm lasers at the flow cell was perpendicular to the FSC-SSC plane. However, this direction of polarization was not maintained at each respective photomultiplier due to intervening fiber optics. Data were subsequently analyzed with no compensation and displayed using FlowJo software (TreeStar Systems, Ashland, OR).

To test the system practically, selected blood samples were manipulated to achieve a low CD4 T-cell percentage near 15%. An R&D Systems, Inc. Human T cell CD8 Subset Column Kit (R&D Systems, Inc., Minneapolis, MN) was used to remove CD8 cells from whole blood. The CD8 cells were then added back to ~400 μL of whole blood, increasing the total CD8 number and decreasing the CD4% of lymphocytes. Samples were prepared with 16 mL whole blood diluted to 35 mL with PBS and underlayed with 15 mL of leukocyte separation medium. Samples were then centrifuged at 3,000 rpm for 15 min. Peripheral blood mononuclear cells (PBMCs) were removed and washed twice with PBS, then centrifuged at 1,500 rpm for 5 min. The protocol for R&D Systems Human T Cell CD8 Subset Column Kit was followed, with the following change: PBMCs from the sample preparation step were removed and suspended in 500 μL of column buffer and mixed with 500 μL of monoclonal antibody cocktail, instead of 1 mL, due to less cells being available for the column than described in the protocol.

Lyophilization

Immunogold at 80 nm diameter conjugated to monoclonal anti-CD4 antibody was obtained in liquid suspension from British Biocell International (British Biocell International, Cardiff, United Kingdom). Aliquots were lyophilized by Quality Bioresources Inc. (Quality Bioresources, Inc., Seguin, Texas) in polypropylene vials with a buffer consisting of stabilizing sugars. The vials contained enough immunogold for 20 tests. For long-term storage, the vials were sealed within foil pouches.

Immunogold CD4 Conjugate Cell Preparation

Lyophilized conjugates of 80 nm colloidal gold and anti-CD4 mouse monoclonal antibody were reconstituted in less than 5 s in distilled water and used for light scatter labeling. Fourteen microliters of reconstituted immunogold were pipetted into the bottom of a polystyrene tube followed by 12 μL of hexadimethrine bromide (Sigma, St. Louis, MO) and 50 μL of K2EDTA whole blood. These three components were vortex mixed at ~1,800 rpm for 45 s to complete the binding

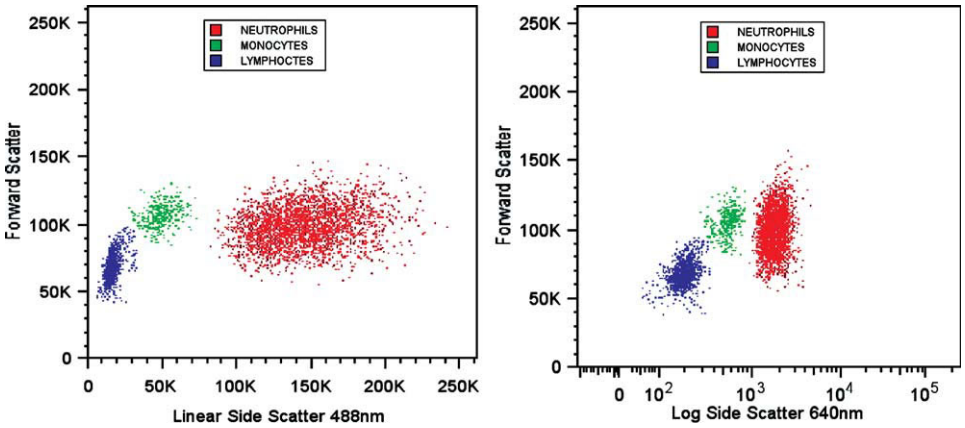

Figure 1. Blood samples without immunogold illustrating the relative placement of lymphocyte, monocyte, and neutrophil clusters gated on SSC and FSC with 488 nm and 640 nm laser illumination. [Color figure can be viewed in the online issue, which is available at wileyonlinelibrary.com.]

reaction. Two mL of isotonic diluent (Avantor, Deventer, Netherlands) was added and mixed by pipette for 5 s. At the final step of preparation, 730 mL of lyse reagent (C2 Diagnostics, Montpellier, France) was added and mixed by pipette for 12 s after which the cells were analyzed immediately on the LSR ll flow cytometer.

Immunogold Flow Cytometric Light Scatter Analysis

SSC was collected from either a 488 nm laser at 100 mW or a 640 nm at 80 mW Coherent Cube laser in which case a Chroma HQ640/10 optical filter (Chroma Technology Corp, Bellows Falls, VT) was used. This optical filter was placed in first position of the trigon filter configuration. SSC and FSC were collected with the identical Diva 6.1 software used throughout this study.

Spectroscopy of Immunogold

Samples of immunogold and samples of aggregated immunogold after combination with hexadimethrine bromide were analyzed for extinction on a Beckman Instruments DU-520 spectrophotometer (Beckman Coulter, Brea, CA) over the wavelength range of 400–1,000 nm.

Microscopy

Samples of buffy coat reacted with immunogold and hexadimethrine bromide were analyzed by oil immersion, transmission light microscopy using an Olympus BHII light microscope (Olympus, Center Valley, PA).

Results

Detection of Immunogold-Labeled Lymphocytes

Normal blood was analyzed by FSC and SSC at 488 nm and at 640 nm using an LSR ll flow cytometer. Control samples without immunogold showed characteristic leukocyte cell clusters for lymphocytes, monocytes, and neutrophils as seen in Figure 1. When cells were labeled with the anti-CD4 immunogold conjugate according to the process described, the lymphocyte cluster split into two clusters as shown in Figure 2. These are consistent with clusters associated with CD4− and CD4+ lymphocyte populations in a normal donor. The

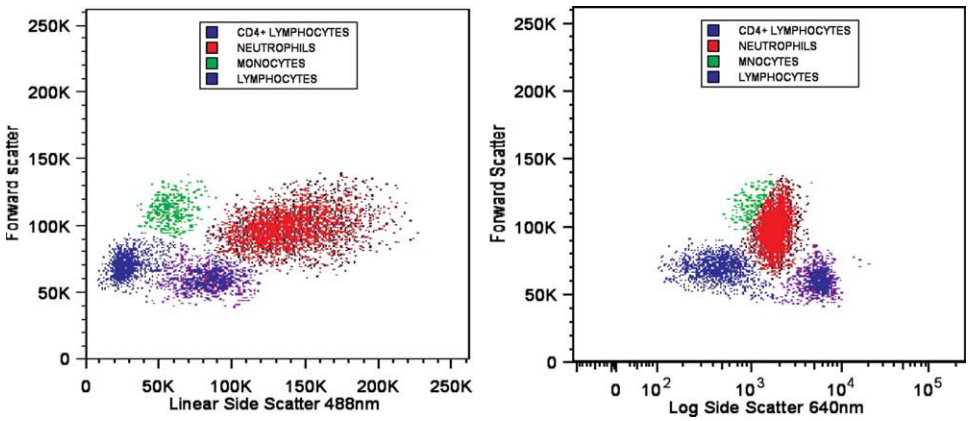

Figure 2. Blood samples labeled with anti-CD4 immunogold conjugates using an ~1 min procedure. With both 488 nm and 640 nm laser illumination, a new cluster defined by increased SSC (granularity) is seen. [Color figure can be viewed in the online issue, which is available at wileyonlinelibrary.com.]

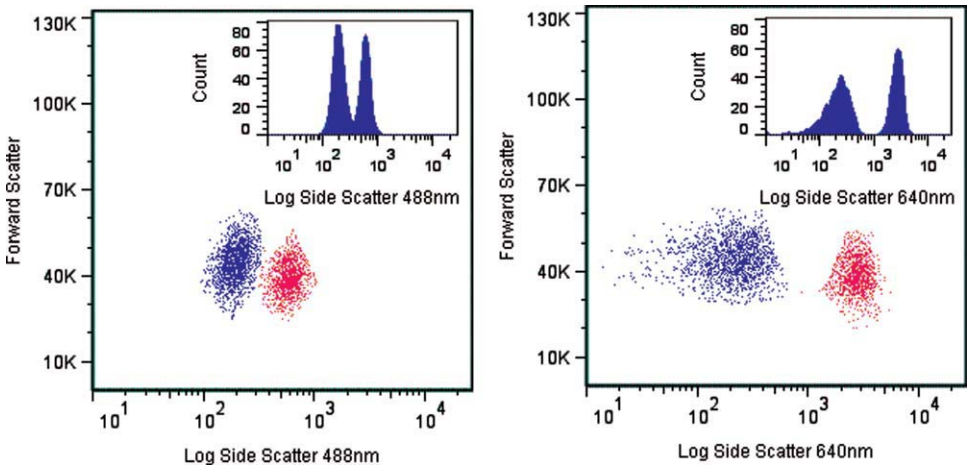

Figure 3. Immunogold-labeled CD4 positive lymphocytes and CD4 negative lymphocytes (gated on SSC and FSC alone) showing significantly greater cluster separation with 640 nm laser illumination compared to 488 nm laser illumination. Gating of lymphocytes is best seen with a linear scale for the 488 nm illumination and log scale for the 640 nm illumintation. The gated results for 488 nm and 640 nm are both shown on a log scale to quantitatively illustrate the greater cluster separation at 640 nm. [Color figure can be viewed in the online issue, which is available at wileyonlinelibrary.com.]

lymphocytes were gated on SSC and FSC at 488 nm and at 640 nm. The CD4 positive lymphocytes were gated on the lymphocyte subpopulation in SSC and FSC. The number of events in the CD4 positive cluster was computed as a percentage of the total number of events in the lymphocyte subpopulation. The results were compared to the CD4% of lymphocytes reported by fluorescence analysis. In this sample, the CD4− cluster was shown by fluorescence to be 59.9% of lymphocytes and shown by immunogold to be 60.0% of lymphocytes. Also, in this sample the CD4+ cluster was shown by fluorescence to be 40.1% of lymphocytes and shown by immunogold to be 40.0% of lymphocytes. The CD4+ cluster showed significantly greater side scatter amplitude due to the presence of the conjugated immunogold and slightly less FSC compared to the CD4− cluster. Normally, CD4+ lymphocytes have less SSC and less FSC than CD4− lymphocytes (6).

The CD4+ lymphocyte cluster was distinct after 45 s of vortex mixing of whole blood, immunogold, and hexadimethrine bromide at 20°C. However, when whole blood and immunogold were vortex mixed and incubated at 20°C without hexadimethrine bromide, an incubation time of more than 2 h was required to produce evidence of the new cluster. This indicates that hexadimethrine bromide plays a significant role in promoting the reaction responsible for creating the immunogold-labeled cluster.

Two wavelength dependent results of immunogold labeling are illustrated in Figures 1 and 2. First, the lymphocyte cluster separation is greater with 640 nm illumination than with 488 nm illumination. With 640 nm illumination, the CD4+ lymphocyte cluster moved to SSC levels that were greater than those for neutrophils. This is further illustrated in Figure 3 where results for blue and red illumination are shown on the same log scale for SSC. With 640 nm illumination, the position of the CD4+ centroid was 15 times the position of the centroid of the CD4− cluster (channel 3384 compared to channel 221). In analyzing the optical physics of immunogold light scatter, it will be important to note later in this report that, using the centroids of the clusters as points of reference, the cluster separation was 4.4 times greater at 640 nm than at 488 nm.

The second wavelength dependent result is the relative transition of the monocyte cluster. All monocytes carry the CD4 surface antigen (at lower density than with lymphocytes), and with 640 nm illumination, the monocyte cluster showed increased SSC and moved into the neutrophil cluster. With 488 nm illumination, the monocyte cluster showed no significant movement to higher levels of SSC.

Comparison of Immunogold at 488 nm and 640 nm

A normal blood sample that had been manipulated to yield a low CD4% as described above was analyzed by fluorescence flow cytometry and by light scatter at 488 nm and 640 nm. Gates on SSC and FSC were constructed for the lymphocyte clusters and the percent of events in the CD4 positive lymphocyte cluster was computed with respect to the total events in lymphocyte cluster (CD4% of lymphocytes) at both wavelengths. These results were compared to the CD4% of lymphocytes reported by fluorescence analysis. Figure 4 shows dot plots for the normal sample where the 488 nm and the 640 nm immunogold results for CD4% were ∼45%, as was the fluorescence flow cytometry result. Figure 5 shows dot plots for the same sample after manipulation to a low CD4% where the 488 nm and the 640 nm immunogold result for CD4% was ∼15%, as was the fluorescence flow cytometry result. Table 1 summarizes replicate measurements on these samples by fluorescence and light scatter. This indicates that CD4% measured by immunogold at 488 nm and 640 nm is consistent between illumination wavelengths and is consistent with fluorescence flow cytometry at normal and low levels.

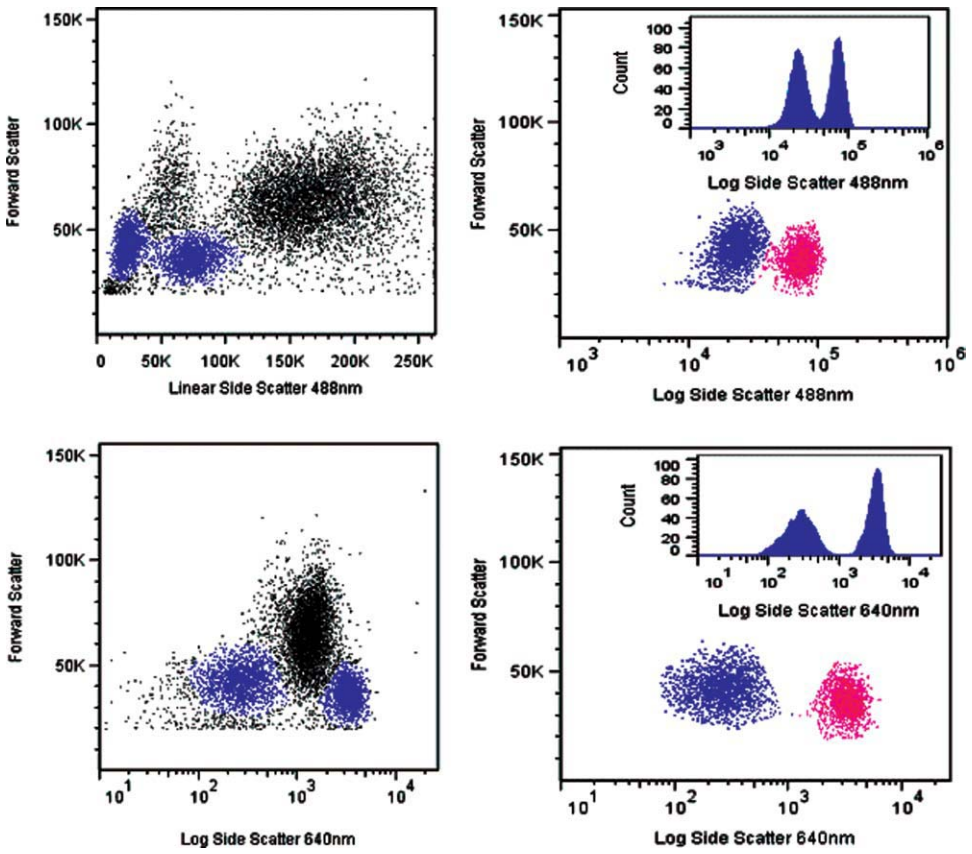

Figure 4. Normal sample illustrating good CD4% agreement between 488 nm (46%) and 640 nm (47%) laser illumination. [Color figure can be viewed in the online issue, which is available at wileyonlinelibrary.com.]

Time to Prepare a Sample for Analysis

A comparison was made for the total time needed to prepare a sample for analysis with the immunogold assay and the fluorescence flow cytometry assay. The fluorescence assay required ~30 min to complete all steps to prepare a sample for analysis, whereas the immunogold assay required ~1 min for completing all steps to prepare the sample for analysis.

Stability of Lyophilized Immunogold Conjugates at High Temperature

To illustrate the stability of lyophilized immunogold, we measured CD4% in normal level control cells (Streck Laboratories, Omaha, NE) using four samples of lyophilized immunogold that had been continuously stored at 42°C (112°F) for 8, 9, 10, 11, and 12 months, respectively. The mean CD4% for the four samples was 52% with a range from 49 to 55%. The trend over these four measurements was less than −0.1% per month. This small degree of variability and absence of a trend indicate good storage stability at temperatures that might be encountered in facilities without refrigeration.

Spectroscopy of Colloidal Gold

Single particle liquid suspensions of 80-nm-diameter immunogold were spectrophotometrically analyzed in for extinction over the wavelength range of 400–1,000 nm. Figure 6a shows a single peak for extinction at a wavelength of 550 nm for this material. When hexadimethrine bromide was added, gold aggregates were created and a shoulder indicative of a second, broader extinction band formed at deep red wavelengths (7). Figure 6b shows a shoulder which is indicative of the formation of this band ~2 s after combining the immunogold and hexadimethrine bromide. A mathematical analysis is presented later in this report to show that an increase in light scatter, and not absorption, is the principal reason for the red extinction band created by hexadimethrine bromide.

Microscopy of Cells

Figure 7 illustrates a lymphocyte following the reaction with immunogold and hexadimethrine bromide. The cell is covered with a granular coat, the appearance of which is consistent with that of aggregated gold particles and inconsistent with a covering of individual, unaggregated 80 nm particles. Being below the limit of visible light resolution, a uniform layer of single 80 nm (0.08 μ) particles would not show granular structure under light microscopy.

Mathematical Light Scatter Analysis

There are two mechanisms for light scatter that affect the SSC signal from immunogold-coated lymphocytes. The first is independent light scatter from each aggregate on the cell

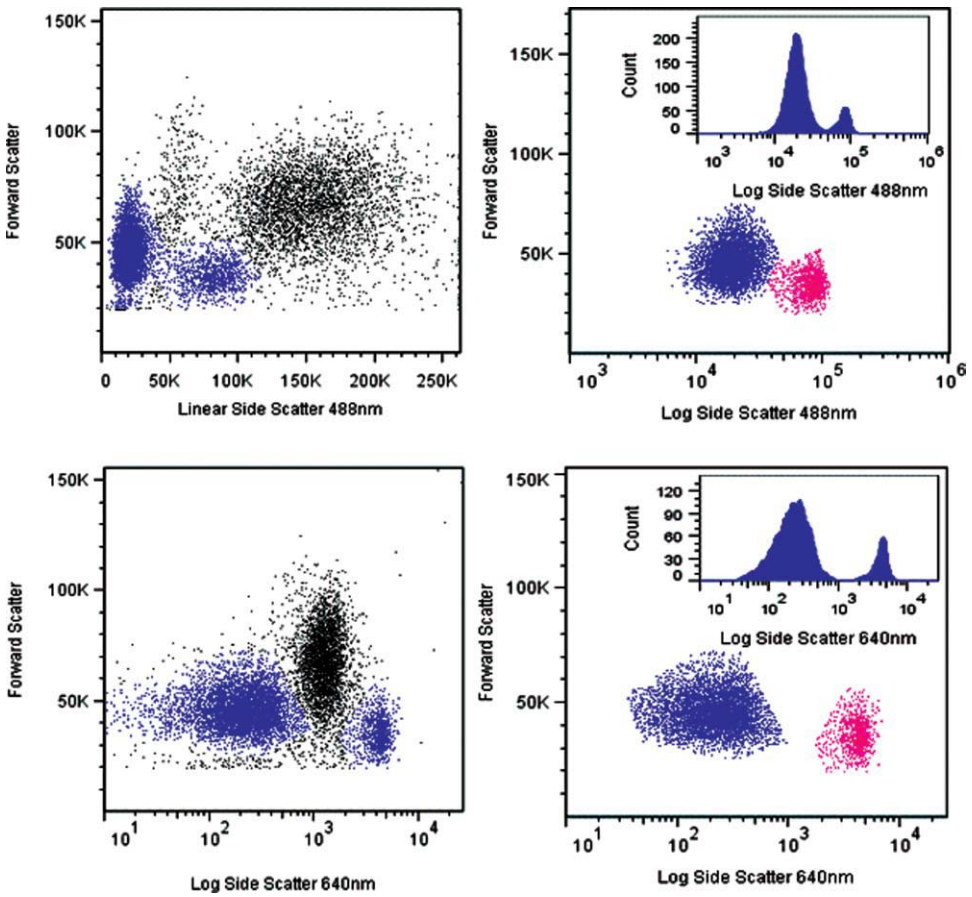

Figure 5. Manipulated sample with low CD4%, illustrating good CD4% agreement between 488 nm (15%) and 640 nm (15%) laser illumination. [Color figure can be viewed in the online issue, which is available at wileyonlinelibrary.com.]

surface, and the second is cooperative light scatter, or "coherent" light scatter from the entire ensemble of aggregates.

Free electron oscillations induced by incoming light in gold particles can resonate and reradiate light (scatter) intensely (8). If there is no phase relationship between the electron oscillations in individual gold particles, then each particle scatters light independently, and as the particles are small, each scatters light in all directions without preference for side scatter. The wavelength, or wavelength band, where resonance occurs depends on the particle size. For gold particles much smaller than the incoming wavelength, the resonant peak is at ~500 nm, and the wavelength for resonance increases toward the red as the particle size increases.

If there is a phase relationship between the electron oscillations in individual gold particles, then scattered light may be strong in directions where individual scattered waves reinforce. This effect is possible with coherent laser light sources but much weaker with incoherent sources such as LEDs.

An analysis follows that computes the relative contribution to enhanced laser light scatter at 640 nm compared to 488 nm coming from optical resonance and from coherent light scatter. MiePlot v4.2.03 software (Philip Laven, Geneva, Switzerland) was used to analyze light scatter from individual gold particles immersed in water. A spatial Fourier Transform method developed by Benedek (9) was used to analyze coherent light scatter from collections of gold particles in water.

Figure 8 is a plot from Mie Theory showing the optical cross sections for absorption and scatter by a 1-μ-diameter gold particle. This is meant to approximately represent a 1 μ diameter aggregate of immunogold as seen in Figure 7 on the surface of a lymphocyte. There is a broad light scatter resonance between 600 nm and 700 nm, whereas there is very little absorption of light in this band. By way of contrast, Figure 9 is

Table 1. CD4% of replicate measurements on low and normal level samples by fluorescence and immunogold light scatter at 488 nm and 640 nm.

	FLUORESCENCE (%)	488 NM IMMUNOGOLD (%)	640 NM IMMUNOGOLD (%)
Low-1	14.7	15.1	15.0
Low-2	14.7	15.0	15.0
Low-3	15.0	15.0	15.0
Normal-1	44.8	46.2	46.5
Normal-2	45.2	43.2	44.9
Normal-3	44.6	44.2	46.7

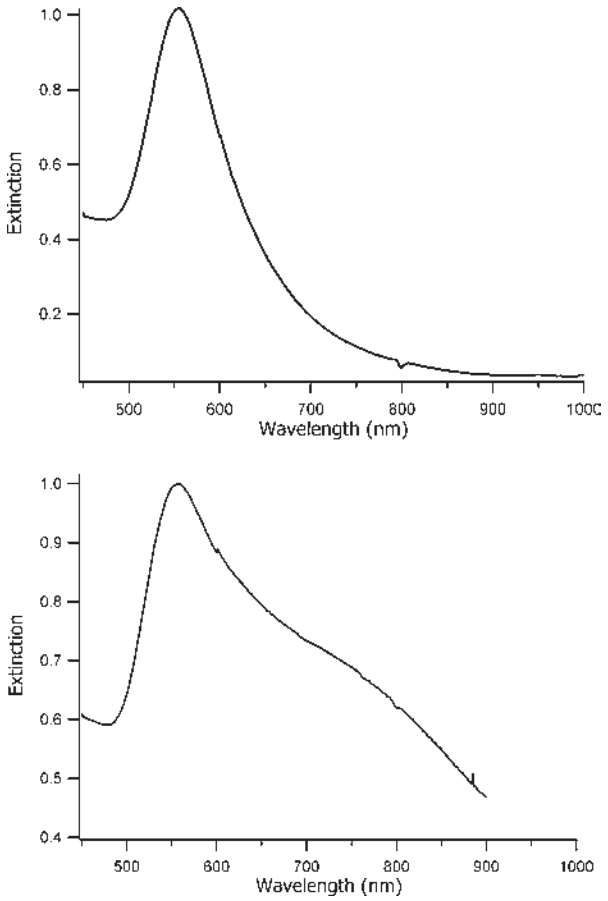

Figure 6. (**a**) Extinction spectroscopy of 80-nm-diameter immunogold particles in aqueous suspension. A clear optical resonance peak is present at 550 nm. (**b**) Extinction spectroscopy of 80-nm immunogold particles immediately after addition of hexadimethrine bromide. The shoulder in the far red is indicative of aggregates.

a plot from Mie Theory showing the optical cross sections for absorption and scatter by an 80-nm-diameter gold particle. The light scatter cross section at 488 nm and 640 nm is two orders of magnitude smaller than is the case for the 1-μ-diameter particle. This implies that aggregates in the 1 μ size range can enhance labeled cell detection by light scatter at 640 nm. For the 1-μ particle, the scatter cross section increases by a factor of 2 between 488 nm and 640 nm.

Although there is an approximate factor of two increase in computed light scatter cross section at 640 nm compared to 488 nm for 1-μ-diameter gold particles, the increase in cluster separation for CD4+/CD4− lymphocytes was approximately a factor of four, which suggests that a second mechanism other than incoherent Mie scatter may be present.

With coherent laser illumination, individual stationary particles do not scatter light independently, but cooperate so as to reinforce scatter over certain ranges of angles while suppressing light scatter over other angular ranges, in much the same mathematical manner as described in Bragg scattering (10). The principle of cooperative or "coherent" light scatter as formulated by Benedek (9) and by Hansen et al. (11) explains why immunogold binding to the cell surface contributes principally to side scatter and little to forward scatter.

It is generally appreciated in flow cytometry that cellular "internal complexity" is the primary source of side scatter. "Internal complexity" refers to irregular distributions of refractive index inside a cell. Adding immunogold clusters to the surface of the cell is optically tantamount to increasing complexity on the cell surface.

The following formula (similar to the equation for Bragg scatter) relates the angular direction Θ for coherent light scatter based on the size Λ of granular structures residing in or on the cells and the wavelength of the laser λ/n in a medium assumed to be water (10).

$$\text{Sin}\ \Theta/2 = \lambda/2n\Lambda \qquad (1)$$

Physically interpreted, Eq. (1) means that spatial variations in optical refractive index with size Λ greater than $\lambda/2n$ are not independent sources of light scatter and sum scattered light coherently in the angular direction Θ.

Immunogold aggregates of a given diameter D give rise to spatially periodic variations in optical refractive index where $D = \Lambda$. Equation (1) predicts that single particles of diameter $D = 0.08\ \mu$ produce periodic variations that are too small to give rise to coherent scatter [(Sin $\Theta/2 > 1$ in Eq. (1)] at either 488 nm or 640 nm. According to Eq. (1), gold particle aggregates up to the 1 μ size seen in Figure 4b will scatter light in a cone from 180° to 20° for 488 nm light and in a cone from 180° to 30° for 640 nm light. SSC collection in flow cytometers spans approximately the angular range of 135°–45°, which includes the angular range for coherent light scatter predicted by

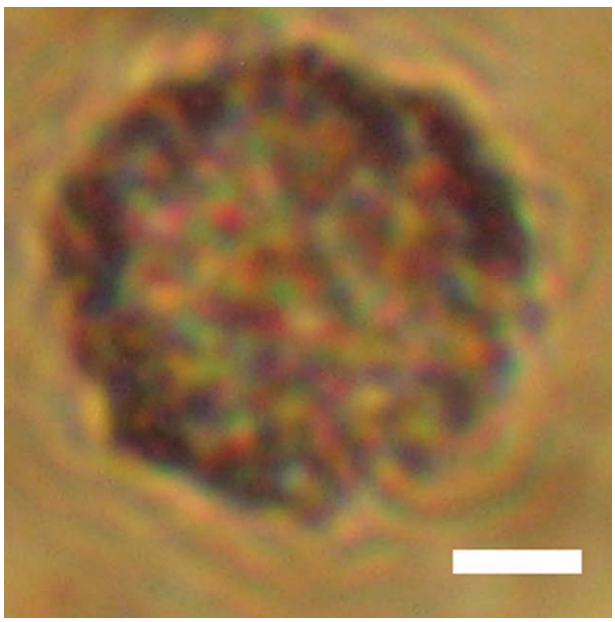

Figure 7. Transmission microscopy of a lymphocyte labeled with immunogold. Aggregates are apparent on the cell surface. Scale is 2 μM. [Color figure can be viewed in the online issue, which is available at wileyonlinelibrary.com.]

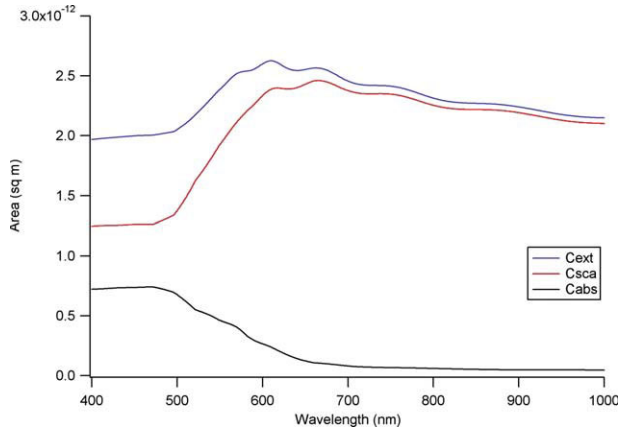

Figure 8. Mie Theory plot of scatter, absorption and extinction optical cross sections for gold particles 1 μ in diameter immersed in water. A broad resonance band is present between 600 nm and 700 nm in the far red. [Color figure can be viewed in the online issue, which is available at wileyonlinelibrary.com.]

Eq. (1). FSC collection in flow cytometers spans the approximate angular range of 0.5°–2°, which is outside the angular range for coherent light scatter predicted by Eq. (1). Thus, coherent light scatter theory predicts that gold particle aggregation would enhance SSC by more than the factor of 2 predicted by incoherent light scatter theory.

As a further confirmation of the importance of coherent light scatter, experimental apparatus was constructed using LED light sources at 460 nm and 640 nm to replace the laser sources. The LED bandwidths were ~50 nm which means that while nominally incoherent, the LED light had a finite coherence length. Equation (2) expresses L_{coh} as a function of LED center wavelength, λ, and wavelength bandwidth, $\Delta\lambda$:

$$L_{coh} = 0.33\ \lambda^2/\Delta\lambda \qquad (2)$$

At 640 nm L_{coh} = 2.7 μ and at 460 nm L_{coh} = 1.4 μ, which means over the dimensions of lymphocytes, which are about 8 μ in diameter, the LED illumination was effectively incoherent.

Figure 10 shows forward scatter and side scatter dot plots obtained using the same sample preparation as was used for the laser studies. The upper dot plot used a 460-nm blue LED source, and the lower dot plot used a 640-nm red LED source. There is an improved cluster separation at 640 nm. The improvement is limited to a factor of 2 as predicted by resonant light scatter from independent particles light scatter, and as would be expected from incoherent sources of light, there is no coherent light scatter contribution.

These comparisons show that the light scatter resonance near 640 nm and the cooperative effects of coherent light scatter with laser illumination each contribute an equal multiplicative factor of 2 to the observed factor of 4 cluster separation improvement observed with 640 nm laser light when compared with 488 nm laser light. These multiplicative factors are independent of laser power, as light scatter intensity is not subject to bleaching or other photo-saturation effects.

Discussion

Three principle results were obtained from this study. First, the cationic surfactant hexadimethrine bromide reduced the time required to label CD4+ lymphocytes with immunogold from over 2 h to less than 1 min. Second, CD4+ cluster separation improved by approximately fourfold when laser light at 640 nm was used compared to laser light at 488 nm. The improvement was by a factor of 2 when incoherent light was used. Third, lyophilized immunogold is active for at least 1 year even when stored continuously at elevated temperatures as high as 42°C.

When hexadimethrine bromide was combined with whole blood and immunogold, the time required to prepare whole blood for light scatter analysis was ~1 min. Without hexadimethrine bromide, the time to bind sufficient immunogold to the cell surface required over 2 h of incubation time. This is best explained by the charge build-up from immunogold particles that have bound to a cell repelling other gold particles as they approach this cell, thus slowing the binding reaction. This inhibition can be overcome by centrifugation as shown by Bohmer and King (1), by long incubation times, or as shown in this study by the addition of a charge neutralization agent. Hexadimethrine bromide has been used to neutralize surface charge on small gold particles that form microstructures in electronics fabrication (12). This cationic surfactant has also been used extensively to neutralize red cell surface charge and enhance weak cell-to-cell binding in red cell antibody testing before blood transfusion (Hexadimethrine bromide is more commonly known as Polybrene in the field of red cell antibody testing). The charge neutralization properties of this surfactant for gold particles and its compatibility with blood cells presented a strong case for its use to reduce the time for immunogold binding in this assay.

The acceleration of the immunogold binding reaction is but one property of hexadimethrine bromide. The other is its apparent ability to create a granular structure of immunogold

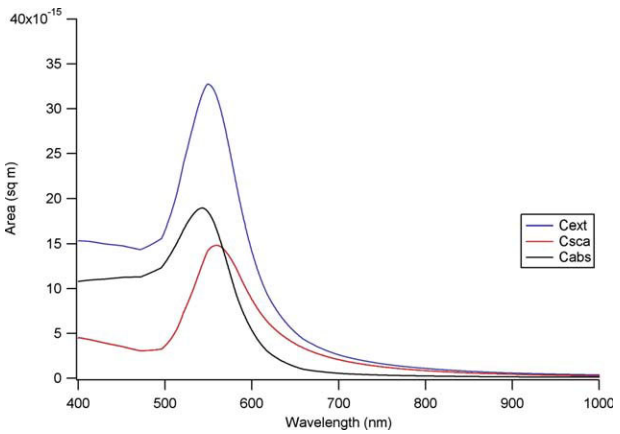

Figure 9. Mie Theory plot of scatter, absorption and extinction optical cross sections for 80-nm gold particles immersed in water. There is good agreement with the extinction spectrum shown in Figure 6a. [Color figure can be viewed in the online issue, which is available at wileyonlinelibrary.com.]

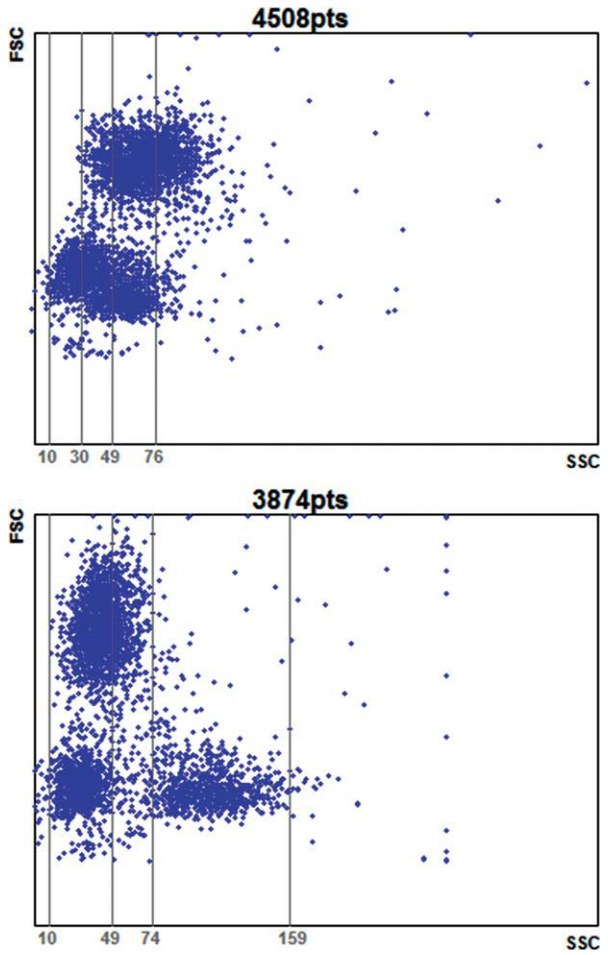

Figure 10. Immunogold-labeled CD4 positive lymphocytes and CD4 negative lymphocytes illuminated by incoherent (LED) light at 460 nm (upper plot) and 640 nm (lower plot). Although the cluster separation is greater with 640 nm illumination, the absence of coherent light scatter limits the improvement in cluster shift to one-half that achieved with coherent (laser) illumination (Fig. 3).

aggregates on the cell surface. Light microscopy revealed aggregates of ~1 μ size (or less) over the surface of ~10-μ-diameter lymphocytes. Smaller aggregates than 1 μ would not be readily resolved by light microscopy but presumably would be present. Aggregates enhance the scattering cross section of the immunogold, shift the wavelength for maximum scatter to the red, and promote wide angle scatter (including side scatter) over other directions of light scatter.

Fluorescent conjugates for flow cytometry require refrigerated shipping and storage at 2 to 8°C. This requirement presents an obstacle to operating flow cytometry facilities in resource challenged regions of the world. It is often estimated that 95% of HIV positive individuals live outside the United States and Europe, and of these approximately two-thirds live in rural communities that often lack reliable refrigeration and are frequently at the end of unstable supply lines. The 1 year stability at 42°C reported here illustrates the high level of heat resistance that can be achieved with immunogold conjugates.

Immunogold has an inherent advantage in this regard over fluorescent conjugates. Reversible lyophilization of a molecule requires an optimum freezing rate, water removal rate, and cryoprotective agents that are generally unique to the molecule. With immunogold conjugates there is but one such molecule, and that is the antibody. With fluorescent conjugate, there are two molecules; the antibody and the fluorochrome. It is difficult to find a common set of freezing rates, water removal rates, and cryoprotective agents that work for both molecules. Thus, metallic particle conjugates are more suitable than fluorescent conjugates insofar as eliminating cold chain shipping and refrigerated storage are concerned.

The fourfold improvement in cluster separation produced by coherent laser illumination at a deep red wavelength has been analyzed and shown to arise partially from the optical resonance in gold particle aggregates of ~1 μ in diameter and partially from a coherent light scatter effect that can only be achieved with lasers. This observation is important for optical designs for immunogold instrumentation where the improvement in cluster separation with a laser source must be weighed against the low noise, robust construction and low cost of incoherent light sources such as LEDs. This is especially important at the point of care.

Our studies have not included polarization effects in immunogold light scatter, and there may be fruitful avenues of study with research flow cytometers where polarization direction can be manipulated. In our study, the LSR II system polarization at 488 nm and 640 nm was perpendicular to the plane of light scatter which is not a direction that would be expected to produce significant wavelength differences in side scatter.

The results reported here have implications for CD4 T-cell analysis in resource poor environments. Light scatter flow cytometry instrumentation is electronically simpler, optically more robust, and less expensive to build than instrumentation for fluorescence flow cytometry and, therefore, has greater potential to be used in difficult settings. Patients who come great distances for CD4 T-cell analysis using substandard and often expensive means of transport are easily discouraged and drop out of HIV management programs when they arrive at the testing site to find that temperature sensitive reagents have been destroyed in shipment and the clinic is closed. Batch analysis methods are used when cell preparation times are long. If 30 min or more is needed for a result, clinics turn to collecting samples in the morning and processing them in a batch manner in the afternoon. Results are not ready until the next day, when patients have returned home. Estimates run as high as 50% for patients who do not return for results.

In addition, these results suggest that other colloidal metals, such as silver, which exhibit resonant surface mode light scatter at other wavelengths (~ 400 nm), might be used in multilaser flow cytometers to enhance data acquisition density. Further study is required to determine whether these conjugates can be used simultaneously with fluorescent conjugates in the presence of hexadimethrine bromide.

Literature Cited

1. Bohmer RM, King NJC. Flow cytometric analysis of immunogold surface label. Cytometry 1984;5:543.
2. Festin R, Bjorklund B, Totterman TH. Detection of triple antibody-binding lymphocytes in standard single laser flow cytometry using colloidal gold, fluorescein and phycoerythrin labels. J Immunol Methods 1987;101:23.
3. Siiman O, Gordon K, Burshteyn A, Maples J, Whitesell J. Immunophenotyping using gold or silver nanoparticle-polystyrene bead conjugates with multiple light scatter. Cytometry 2000;41:298–307.
4. Crow MJ, Marinakos SM, Cook JM, Chilkoti A, Wax A. Plasmonic flow cytometry by immunolabeled nanorods. Cytometry Part A 2011;79A:57–65.
5. Preffer FI, Dombkowski DD. Advances in complex multiparameter flow cytometry technology: Applications in stem cell research. Cytometry Part B 2009;76B:295–314.
6. Olson D, Kelliher A, Dombkowski D, Preffer F. Clinical monitoring of transplant immunomodulation: Immunosuppression and T-cell clearance with the anti-CD3 monoclonal antibody OKT. In: Robinson P, editor. The Purdue University Cytometry Laboratories CD-ROM, Vol.5. West Lafayette, IN; 2000.
7. Norman TJ, Grant CD, Magana D, Zhang JZ, Liu J, Cao D, Bridges F, Van Buuren A. Near infrared optical absorption of gold particle aggregates. J Phys Chem B 2002;106:7005–7012.
8. Bohren CF, Huffman DR. Absorption and Scattering of Light by Small Particles. New York: Wiley; 1983. Chapter 12.
9. Benedek G. Theory of transparency of the eye. Appl Opt 1971;10:459.
10. Kittel C. Introduction to Solid State Physics. Hoboken, NJ: Wiley; 2005. p 25.
11. Hansen W, Hoffman R, Ip S, Healy K. Light scatter as an adjunct to cellular immunofluorescence in flow cytometric systems. J Clin Immunol 1982;2:32S.
12. Tien J, Terfort A, Whitesides G. Microfabrication through electrostatic self-assembly. Langmuir 1997;13:5349.